



**HAL**  
open science

## Subspace method for continuous-time fractional system identification

Magalie Thomassin, Rachid R. Malti

► **To cite this version:**

Magalie Thomassin, Rachid R. Malti. Subspace method for continuous-time fractional system identification. 15th IFAC Symposium on System Identification, SYSID 2009, Jul 2009, Saint Malo, France. pp.TuA3.6. hal-00383811

**HAL Id: hal-00383811**

**<https://hal.science/hal-00383811>**

Submitted on 13 May 2009

**HAL** is a multi-disciplinary open access archive for the deposit and dissemination of scientific research documents, whether they are published or not. The documents may come from teaching and research institutions in France or abroad, or from public or private research centers.

L'archive ouverte pluridisciplinaire **HAL**, est destinée au dépôt et à la diffusion de documents scientifiques de niveau recherche, publiés ou non, émanant des établissements d'enseignement et de recherche français ou étrangers, des laboratoires publics ou privés.

# Subspace method for continuous-time fractional system identification

Magalie Thomassin, Rachid Malti

*Université de Bordeaux, IMS, CNRS UMR 5218, 351 cours de la  
libération, 33405 Talence Cedex, France (e-mail:  
{magalie.thomassin,rachid.malti}@ims-bordeaux.fr)*

---

**Abstract:** The aim of this paper is to develop a subspace method for state-space identification of continuous-time systems using fractional commensurate models. As compared to the classical state-space representation, the commensurate differentiation order must be estimated besides the state-space matrices. The latter are estimated with conventional subspace-based techniques using QR and singular value decompositions, whereas the commensurate order is estimated using nonlinear programming. This is the first method developed for multi-input multi-output system identification of fractional models. The performances are demonstrated by simulations at various signal-to-noise ratios assuming a known then an unknown commensurate order.

Keywords: Fractional state-space representation, continuous-time identification, subspace method, multivariable model.

---

## 1. INTRODUCTION

Fractional models have witnessed a growing interest during the last years. Many diffusive phenomena can be modeled by fractional transfer functions. In electrochemistry for instance, diffusion of charges in acid batteries is governed by Randles models [Sabatier et al. (2006)] that involve Warburg impedance with an integrator of order 0.5. Electrochemical diffusion showed to have a tight relation with derivatives of order 0.5 [Oldham and Spanier (1973)]. In thermal diffusion of a semi-infinite homogeneous medium, Battaglia et al. (2001) have shown that the exact solution of the heat equation links thermal flux to a half order derivative of the surface temperature on which the flux is applied.

Time-domain system identification using fractional models was initiated in the late nineties. Oustaloup et al. (1996) developed a method based on the discretization of the fractional differential equation using Grünwald definition and on the estimation of its coefficients using least squares. Trigeassou et al. (1999) based their identification method on the approximation of a fractional integrator by a rational model. Then, they deduced the fractional model after estimating its rational approximation. Cois et al. (2001) proposed several extensions of equation error methods, such as the state variable filters and the instrumental variable (IV), to fractional system identification. Aoun et al. (2007) synthesized fractional orthogonal bases generalizing various bases (Laguerre, Kautz,...) to fractional differentiation orders for identification issues. Recently, Malti et al. (2008b) have extended the concept of optimal IV methods to fractional systems. For an overview of these identification methods refer to Malti et al. (2008a).

In this paper, we consider the problem of identifying a continuous-time (CT) fractional system in its state-space form. Only few papers deal with system identification us-

ing fractional state-space representation [Cois et al. (2001); Pointot and Trigeassou (2004)]. They are based on the minimization of an output error criterion by nonlinear programming. These methods are well suited for single-input single-output (SISO) systems, and are generally difficult to apply in the multi-input multi-output (MIMO) case because the number of parameters to estimate becomes large. Here, a subspace method to estimate the matrices of the CT fractional state-space representation is proposed. It is an extension of the methods presented in the literature for rational systems [Haverkamp et al. (1996); Johansson et al. (1997, 1999)] to the fractional ones. Other subspace techniques for identifying CT systems with rational models can be found in Bastogne et al. (2001); Ohsumi et al. (2002); Mercère et al. (2007). So, the proposed method inherits the advantages of subspace methods which stem from the reliability of the numerical algorithms using the QR and the singular value decompositions [Katayama (2005)]. Thus, it does not involve nonlinear optimization to obtain state-space matrices. In addition, no canonical form (such as modal or companion) of the state-space representation is required. Finally, the proposed subspace algorithms can be applied to the identification of both SISO and MIMO fractional systems. As will be seen later, the state-space representation of a fractional commensurate system involves an additional parameter which is the commensurate order. This parameter is the only one computed by minimizing an output error criterion with a nonlinear optimization technique.

In section 2, some recalls about fractional systems are given. Section 3 presents the method proposed to estimate the matrices of the CT fractional state-space representation, followed by simulation examples in Section 4. Finally, Section 5 is devoted to the estimation of the fractional commensurate order. Monte Carlo simulations are made to check the statistical properties of the estimator.

## 2. FRACTIONAL SYSTEMS

The concept of differentiation to an arbitrary non-integer order  $\alpha$ , with  $\alpha \in \mathbb{R}^{+*}$  (set of strictly positive real numbers),  $\mathcal{D}^\alpha \triangleq \left(\frac{d}{dt}\right)^\alpha$ , was defined in the 19<sup>th</sup> century by Riemann and Liouville. The  $\alpha$ -order fractional derivative of  $f(t)$  is defined as an integer derivative of order  $[\alpha] + 1$  ( $[\cdot]$  stands for the floor operator) of a non-integer integral of order  $\alpha - [\alpha]$  [Samko et al. (1993)]:

$$\mathcal{D}^\alpha f(t) = \frac{d^{[\alpha]+1}}{dt^{[\alpha]+1}} \left\{ \frac{1}{\Gamma([\alpha] + 1 - \alpha)} \int_0^t \frac{f(\tau)}{(t - \tau)^{\alpha - [\alpha]}} d\tau \right\}$$

where the Euler gamma function  $\Gamma(\beta)$  is defined for every  $\beta \in \mathbb{R}^{+*}$  by:

$$\Gamma(\beta) = \int_0^\infty z^{\beta-1} e^{-z} dz.$$

The Laplace transform, denoted by  $\mathcal{L}$ , is a more concise algebraic tool which allows to write, in case of zero initial conditions, [Oldham and Spanier (1974)]:

$$\mathcal{L}\{\mathcal{D}^\alpha f(t)\} = s^\alpha F(s), \text{ with } F(s) \triangleq \mathcal{L}\{f(t)\}$$

where  $s$  is the Laplace variable.

A SISO fractional system is governed by a fractional differential equation:

$$y(t) + a_1 \mathcal{D}^{\alpha_1} y(t) + \dots + a_{m_A} \mathcal{D}^{\alpha_{m_A}} y(t) = b_0 \mathcal{D}^{\beta_0} u(t) + b_1 \mathcal{D}^{\beta_1} u(t) + \dots + b_{m_B} \mathcal{D}^{\beta_{m_B}} u(t)$$

where  $(a_j, b_i) \in \mathbb{R}^2$ , and the differentiation orders  $\alpha_1 < \alpha_2 < \dots < \alpha_{m_A}$ ,  $\beta_0 < \beta_1 < \dots < \beta_{m_B}$  are allowed to be non-integer positive numbers. State space representation was extended by Matignon and d'Andréa Novel (1996) to commensurate fractional systems, where all the differentiation orders are multiple integers of  $\alpha$ . The extension was done by allowing the differentiation order of the state vector to be any commensurate order  $\alpha \in \mathbb{R}^{+*}$ . The fractional state space representation is presented in a MIMO case as:

$$\mathcal{D}^\alpha \mathbf{x}(t) = \mathbf{A}\mathbf{x}(t) + \mathbf{B}\mathbf{u}(t), \quad (1)$$

$$\mathbf{y}(t) = \mathbf{C}\mathbf{x}(t) + \mathbf{D}\mathbf{u}(t) \quad (2)$$

where  $\mathbf{x} \in \mathbb{R}^n$  is the state vector,  $\mathbf{u} \in \mathbb{R}^m$  the input vector,  $\mathbf{y} \in \mathbb{R}^p$  the output vector,  $\mathbf{A} \in \mathbb{R}^{n \times n}$ ,  $\mathbf{B} \in \mathbb{R}^{n \times m}$ ,  $\mathbf{C} \in \mathbb{R}^{p \times n}$ ,  $\mathbf{D} \in \mathbb{R}^{p \times m}$  are constant matrices. Zero initial conditions are considered:  $\mathbf{x}(t) = 0$  for  $t \leq 0$ . Matignon (1998) proved that the fractional system (1)-(2) is stable if and only if:

$$0 < \alpha < 2 \quad \text{and} \quad |\arg(\lambda_k)| > \frac{\pi}{2} \quad \forall k = 1, \dots, n$$

where  $\lambda_k$  is the  $k^{\text{th}}$ -eigenvalue of  $\mathbf{A}$  and  $|\arg(\lambda_k)| \leq \pi$ .

The conversion of (1)-(2) to the MIMO transfer function form is obtained as for the rational systems by:

$$G(s) = C(s^\alpha I - A)^{-1} B + D.$$

In the following, assume that  $(A, B)$  is reachable and  $(C, A)$  is observable. The controllability and the observability conditions of a state space representation of a commensurate fractional system are the same as for rational systems [Matignon and d'Andréa Novel (1996)].

One of the main difficulties with fractional models is the time-domain simulation. This problem has been extensively studied and an overview of the principal methods can be found in Aoun et al. (2004). The most commonly used approximation of fractional operators is the recursive

distribution of zeros and poles, proposed by Oustaloup (1995), which approximates the frequency behavior of  $s^\alpha$  in the frequency range  $[\omega_A, \omega_B]$ . Nevertheless, this approximation has null asymptotic behaviors at low and high frequencies, which can introduce a static error between the fractional model and its approximation. To avoid this drawback, Trigeassou et al. (1999) suggested to use the conventional integrator outside the frequency range  $[\omega_A, \omega_B]$ :

$$s_{[\omega_A, \omega_B]}^{-\alpha} = \frac{G_\alpha}{s} \prod_{k=1}^{N_c} \frac{1 + s/\omega'_k}{1 + s/\omega_k} \quad (3)$$

where:

- $N_c$  is the number of cells (directly related to the quality of the approximation),
- $G_\alpha$  is fixed so that  $s^{-\alpha}$  has the same gain as  $s_{[\omega_A, \omega_B]}^{-\alpha}$  in the middle of the interval  $[\omega_A, \omega_B]$ ,
- $\omega'_k$  and  $\omega_k$  are respectively zeros and poles recursively distributed in the frequency range  $[\omega_b, \omega_h] = [\sigma^{-1}\omega_A, \sigma\omega_B]$  where  $\sigma$  is generally set to 10 to minimize border effects. They are defined by the following relations:

$$\omega'_k = \gamma\omega_k, \quad \omega_{k+1} = \eta\omega'_k, \quad \alpha = 1 - \frac{\log \gamma}{\log \eta}.$$

This approximation is used to simulate the fractional systems presented in this paper with the parameters:  $N_c = 20$ ,  $\omega_A = 10^{-5}$  and  $\omega_B = 10^5$ .

## 3. SUBSPACE ALGORITHMS FOR FRACTIONAL STATE-SPACE IDENTIFICATION

Consider the linear CT fractional state-space representation (1)-(2). The problem in this section is to estimate the system matrices  $A$ ,  $B$ ,  $C$ ,  $D$  from sampled input-output data<sup>1</sup>  $\{\mathbf{u}_k\}_{k=0}^{N-1}$  and  $\{\mathbf{y}_k\}_{k=0}^{N-1}$ . The commensurate order  $\alpha$  is assumed to be known. The case where  $\alpha$  is unknown will be discussed in section 5.

The Laplace transform of (1)-(2) gives:

$$s^\alpha X(s) = AX(s) + BU(s) \quad (4)$$

$$Y(s) = CX(s) + DU(s). \quad (5)$$

The problem in these relations is the use of the  $s^\alpha$ -operator which amplifies noise in the time domain, especially at high frequencies. To avoid this problem, the low-pass filter:

$$\lambda = \frac{1}{1 + \left(\frac{s}{\omega_f}\right)^\alpha} = \frac{1}{1 + \tau s^\alpha} \text{ with } \tau = (1/\omega_f)^\alpha \quad (6)$$

is introduced. Then, (4) is transformed into:

$$X(s) = A_\lambda[\lambda X(s)] + B_\lambda[\lambda U(s)] \quad (7)$$

with  $A_\lambda = I + \tau A$  and  $B_\lambda = \tau B$ . Application of the inverse Laplace transform leads to the following system of linear equations:

$$\mathbf{x}(t) = A_\lambda[\lambda \mathbf{x}(t)] + B_\lambda[\lambda \mathbf{u}(t)] \quad (8)$$

$$\mathbf{y}(t) = C\mathbf{x}(t) + \mathbf{D}\mathbf{u}(t) \quad (9)$$

where  $\lambda \mathbf{x}(t)$  and  $\lambda \mathbf{u}(t)$  correspond to the states and the inputs prefiltered by  $\lambda$  in (6). Then, from (9), it is found by recursion that:

<sup>1</sup> The discrete-time variables are denoted by  $x_k$  and correspond to the time sampling with a constant sampling period  $T_s$  of the CT variable  $x(t)$ :  $x_k = x(kT_s)$ .

$$\begin{aligned}
\mathbf{y}(t) &= C\mathbf{x}(t) + D\mathbf{u}(t) \\
&= CA_\lambda[\lambda\mathbf{x}(t)] + CB_\lambda[\lambda\mathbf{u}(t)] + D\mathbf{u}(t) \\
&\quad \vdots \\
&= CA_\lambda^k[\lambda^k\mathbf{x}(t)] + \sum_{j=1}^k CA_\lambda^{k-j}B_\lambda[\lambda^{k-j+1}\mathbf{u}(t)] + D\mathbf{u}(t)
\end{aligned}$$

for  $k \in \mathbb{N}^*$ , where  $\lambda^k\mathbf{x}(t)$  denotes the signals obtained from  $\mathbf{x}(t)$  by filtering through a series of  $k$  low-pass filters  $\lambda$ . In the same way, it is found for  $l \in \mathbb{N}^*$ :

$$\begin{aligned}
\lambda^l\mathbf{y}(t) &= C\lambda^l\mathbf{x}(t) + D\lambda^l\mathbf{u}(t) \\
&= CA_\lambda[\lambda^{l+1}\mathbf{x}(t)] + CB_\lambda[\lambda^{l+1}\mathbf{u}(t)] + D\mathbf{u}(t) \\
&\quad \vdots \\
&= CA_\lambda^{k-l}[\lambda^k\mathbf{x}(t)] + \sum_{j=1}^{k-l} CA_\lambda^{k-j-l}B_\lambda[\lambda^{k-j+1}\mathbf{u}(t)] \\
&\quad + D\mathbf{u}(t)
\end{aligned}$$

with  $k \geq l$ . As a consequence, the input-output data can be formulated as the following extended linear model:

$$\mathcal{Y}(t) = \mathcal{O}_i \mathcal{X}(t) + \Psi_i U(t) \quad (10)$$

with input-output and state variables:

$$\mathcal{Y}(t) = \begin{bmatrix} \lambda^{i-1}\mathbf{y}(t) \\ \lambda^{i-2}\mathbf{y}(t) \\ \vdots \\ \lambda^1\mathbf{y}(t) \\ \mathbf{y}(t) \end{bmatrix}, \quad U(t) = \begin{bmatrix} \lambda^{i-1}\mathbf{u}(t) \\ \lambda^{i-2}\mathbf{u}(t) \\ \vdots \\ \lambda^1\mathbf{u}(t) \\ \mathbf{u}(t) \end{bmatrix}, \quad \mathcal{X}(t) = \lambda^{i-1}\mathbf{x}(t)$$

and:

$$\mathcal{O}_i = \begin{bmatrix} C \\ CA_\lambda \\ \vdots \\ CA_\lambda^{i-1} \end{bmatrix}, \quad \Psi_i = \begin{bmatrix} D & 0 & \cdots & 0 \\ CB_\lambda & D & \ddots & \vdots \\ \vdots & \ddots & \ddots & 0 \\ CA_\lambda^{i-2}B_\lambda & \cdots & CB_\lambda & D \end{bmatrix}$$

where  $\mathcal{O}_i \in \mathbb{R}^{ip \times n}$  is the extended observability matrix and  $\Psi_i \in \mathbb{R}^{ip \times im}$  is a block Toeplitz matrix. Now, from  $N$  input-output available samples observed at discrete times  $t_k = kT_s$  for  $k = 0, \dots, N-1$ , the extended linear model (10) can be rewritten as:

$$\mathcal{Y}_N = \mathcal{O}_i \mathcal{X}_N + \Psi_i U_N \quad (11)$$

where

$$U_N = \begin{bmatrix} [\lambda^{i-1}\mathbf{u}]_0 & [\lambda^{i-1}\mathbf{u}]_1 & \cdots & [\lambda^{i-1}\mathbf{u}]_{N-1} \\ [\lambda^{i-2}\mathbf{u}]_0 & [\lambda^{i-2}\mathbf{u}]_1 & \cdots & [\lambda^{i-2}\mathbf{u}]_{N-1} \\ \vdots & \vdots & \ddots & \vdots \\ [\lambda\mathbf{u}]_0 & [\lambda\mathbf{u}]_1 & \cdots & [\lambda\mathbf{u}]_{N-1} \\ \mathbf{u}_0 & \mathbf{u}_1 & \cdots & \mathbf{u}_{N-1} \end{bmatrix} \in \mathbb{R}^{mi \times N}$$

by using the following notation for sampled filtered data:

$$[\lambda^j\mathbf{u}]_k = \lambda^j\mathbf{u}(t_k). \quad (12)$$

The matrices  $\mathcal{Y}_N \in \mathbb{R}^{pi \times N}$  and  $\mathcal{X}_N \in \mathbb{R}^{n \times N}$  are constructed in a similar way. Equation (11) enables to use subspace identification algorithms as in their original non-fractional discrete-time version. We have chosen to use the ordinary MOESP (MIMO Output-Error State Space) algorithm [Katayama (2005)]. The principle of this algorithm is as follows:

(1) Compute an LQ decomposition of the data matrix:

$$\begin{bmatrix} \mathcal{U}_N \\ \mathcal{Y}_N \end{bmatrix} = \begin{bmatrix} L_{11} & 0 \\ L_{21} & L_{22} \end{bmatrix} \begin{bmatrix} Q_1^T \\ Q_2^T \end{bmatrix} \quad (13)$$

where  $L_{11} \in \mathbb{R}^{im \times im}$ ,  $L_{21} \in \mathbb{R}^{ip \times im}$ ,  $L_{22} \in \mathbb{R}^{ip \times ip}$  with  $L_{11}$ ,  $L_{22}$  lower triangular, and  $Q_1 \in \mathbb{R}^{N \times im}$ ,  $Q_2 \in \mathbb{R}^{N \times ip}$  are orthogonal.

(2) Compute a singular value decomposition (SVD) of the  $L_{22}$  matrix approximating the column space of  $\mathcal{O}_i$ :

$$L_{22} = [U_1 \ U_2] \begin{bmatrix} \Sigma_1 & 0 \\ 0 & 0 \end{bmatrix} \begin{bmatrix} V_1^T \\ V_2^T \end{bmatrix} \quad (14)$$

where  $U_1 \in \mathbb{R}^{ip \times n}$  and  $U_2 \in \mathbb{R}^{ip \times (ip-n)}$ . The state order  $n$  can be estimated from the SVD since  $n = \dim \Sigma_1$  in the noiseless case.

(3) Estimate the extended observability matrix:

$$\hat{\mathcal{O}}_i = U_1 \Sigma_1^{1/2}. \quad (15)$$

(4) Estimate the  $C$  matrix:  $\hat{C} = \hat{\mathcal{O}}_i(1 : p, 1 : n)$ .

(5) Estimate  $A_\lambda$  by solving the linear equation:

$$\hat{\mathcal{O}}_i(1 : p(i-1), 1 : n) A_\lambda = \hat{\mathcal{O}}_i(p+1 : ip, 1 : n). \quad (16)$$

(6) Estimate the  $B_\lambda$  and  $D$  matrices. For that purpose, it can be shown that:

$$U_2^T \Psi_i = U_2^T L_{21} L_{11}^{-1} \quad (17)$$

which is a linear equation with respect to  $B_\lambda$  and  $D$ . Define:

$$U_2^T \triangleq [\mathcal{L}_1 \ \mathcal{L}_2 \ \cdots \ \mathcal{L}_i] \quad (18)$$

$$U_2^T L_{21} L_{11}^{-1} \triangleq [\mathcal{M}_1 \ \mathcal{M}_2 \ \cdots \ \mathcal{M}_i] \quad (19)$$

with  $\mathcal{L}_k \in \mathbb{R}^{(ip-n) \times p}$  and  $\mathcal{M}_k \in \mathbb{R}^{(ip-n) \times m}$  for  $k = 1, \dots, i$ . Thus, from (17):

$$\mathcal{L}_1 D + \mathcal{L}_2 \hat{C} D + \cdots + \mathcal{L}_i \hat{C} \hat{A}_\lambda^{i-2} B_\lambda = \mathcal{M}_1$$

$$\mathcal{L}_2 D + \mathcal{L}_3 \hat{C} D + \cdots + \mathcal{L}_i \hat{C} \hat{A}_\lambda^{i-3} B_\lambda = \mathcal{M}_2$$

$\vdots$

$$\mathcal{L}_{i-1} D + \mathcal{L}_i \hat{C} D = \mathcal{M}_{i-1}$$

$$\mathcal{L}_i D = \mathcal{M}_i.$$

Define  $\bar{\mathcal{L}}_k = [\mathcal{L}_k \ \cdots \ \mathcal{L}_i] \in \mathbb{R}^{(ip-n) \times (i+1-k)p}$ ,  $k = 2, \dots, i$ , and get the following overdetermined system of linear equations:

$$\begin{bmatrix} \mathcal{L}_1 & \bar{\mathcal{L}}_2 \hat{\mathcal{O}}_{i-1} \\ \mathcal{L}_2 & \bar{\mathcal{L}}_3 \hat{\mathcal{O}}_{i-2} \\ \vdots & \vdots \\ \mathcal{L}_{i-1} & \bar{\mathcal{L}}_i \hat{\mathcal{O}}_1 \\ \mathcal{L}_i & 0 \end{bmatrix} \begin{bmatrix} D \\ B_\lambda \end{bmatrix} = \begin{bmatrix} \mathcal{M}_1 \\ \mathcal{M}_2 \\ \vdots \\ \mathcal{M}_{i-1} \\ \mathcal{M}_i \end{bmatrix} \quad (20)$$

where the block coefficient matrix in the left-hand side is of dimensions  $i(ip-n) \times (p+n)$ . Estimates of  $B_\lambda$  and  $D$  are estimated by finding the least-squares solution of (20).

The matrices of the fractional CT state-space representation (4)-(5) are then deduced as follows:  $\hat{A} = \frac{1}{\tau}(\hat{A}_\lambda - I)$ ,  $\hat{B} = \frac{1}{\tau}\hat{B}_\lambda$ . The  $\hat{C}$  and  $\hat{D}$  matrices do not change.

#### 4. EXAMPLE

The algorithm is applied to input-output data of length  $N = 1023$  generated by simulating the linear system (1)-(2) with  $\alpha = 0.9$ ,

$$A = \begin{bmatrix} 0 & -0.1 \\ 1 & -0.2 \end{bmatrix}, B = \begin{bmatrix} 1 \\ 0 \end{bmatrix}, C = \begin{bmatrix} 0 & 0.1 \\ 0.5 & -0.1 \end{bmatrix}, D = \begin{bmatrix} 0 \\ 0 \end{bmatrix},$$

and zero initial conditions. The input signal is a pseudorandom binary sequence (PRBS) with maximum length. The sampling period is  $T_s = 0.05s$ . The outputs (Fig. 1) are corrupted by white noise with a signal-to-noise ratio (SNR) of 20 dB. The algorithm parameters are set to  $i = 8$

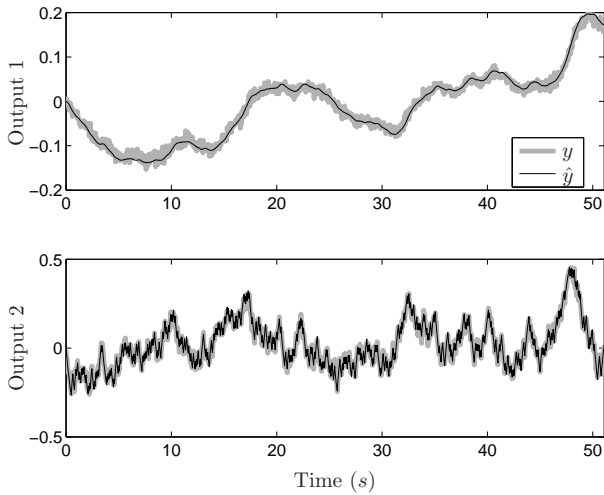


Fig. 1. Output data  $y$  and output of the estimated model  $\hat{y}$  for a PRBS as input (SNR=20 dB).

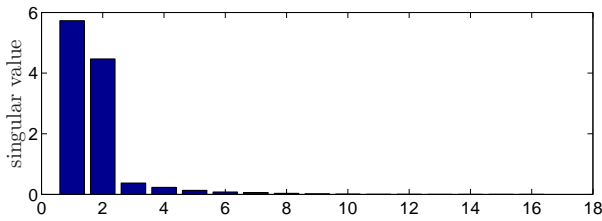


Fig. 2. The 16 ( $= ip$ ) singular values of  $L_{22}$  ( $\hat{n} = 2$ ).

and  $\omega_f = 6$  and the commensurate order  $\alpha$  is set to its true value. In these conditions, a second-order state-space representation is estimated with a good accuracy with the following companion form:

$$\hat{A} = \begin{bmatrix} 0 & -0.0984 \\ 1 & -0.1853 \end{bmatrix}, \hat{B} = \begin{bmatrix} 1 \\ 0 \end{bmatrix},$$

$$\hat{C} = \begin{bmatrix} 0.0002 & 0.1015 \\ 0.5114 & -0.0962 \end{bmatrix}, \hat{D} = \begin{bmatrix} 0.0004 \\ 0.0024 \end{bmatrix}.$$

The estimated outputs  $\hat{y}$  are plotted in Fig. 1. The normalized prediction error norm ( $\|\hat{y} - y\|_2 / \|y\|_2$ ) equals 0.1109 (-19.1 dB) for the first output and 0.1082 (-19.3 dB) for the second one. The singular values of  $L_{22}$  are plotted in Fig. 2. The state-space order was easily deduced since we observe an abrupt change at  $\hat{n} = 2$ . Different order estimation criteria may also be used [Bauer (2001)].

Fig. 3 shows the influence of the method parameters (the number of block rows  $i$  and the filter frequency  $\omega_f$ ) on the normalized error norm  $\|\hat{y} - y\|_2 / \|y\|_2$  for the first output (similar results are obtained with the second output). The estimation is considered incorrect if the normalized error norm is greater than or equal to one (*i.e.* if its logarithm is greater than or equal to zero). So, in Fig. 3, all normalized errors greater than one are set to one. These figures also show the sensitivity to stochastic disturbance by considering various SNRs: 20, 15 and 10 dB. The contour levels indicate that  $\omega_f$  can be chosen in a suitable range over one decade, between 1 and 10 for a SNR greater than 15 dB. In the case of a higher noise level, this range is slightly reduced and the choice of  $i$  acts more on the results: fine results are obtained from  $i = 6$  with  $\omega_f \in [3, 10]$  for SNR=10 dB.

To analyze the estimator statistical properties, 500 data sets, each with different realization of the noise, are generated for three SNRs (20, 15 and 10 dB). The means of the normalized error norms, obtained with  $i = 8$  and  $\omega_f = 6$ , are given in table 1 and Fig. 4 shows the estimated poles. The normalized mean squared error (MSE) of the poles are indicated in table 2. It can be seen that the estimator is biased. Indeed, the persistent excitation of the input, obtained with a PRBS for example, may not be enough to guarantee the consistency of the estimates for MOESP [Bauer and Jansson (2000)].

Table 1. Means of the normalized error norms over 500 runs ( $\alpha$  known).

	output	SNR=20 dB	SNR=15 dB	SNR=10 dB
mean of the normalized error norm	1	0.1041 (-19.66 dB)	0.1859 (-14.62 dB)	0.3414 (-9.34 dB)
	2	0.1032 (-19.72 dB)	0.1846 (-14.67 dB)	0.3419 (-9.32 dB)

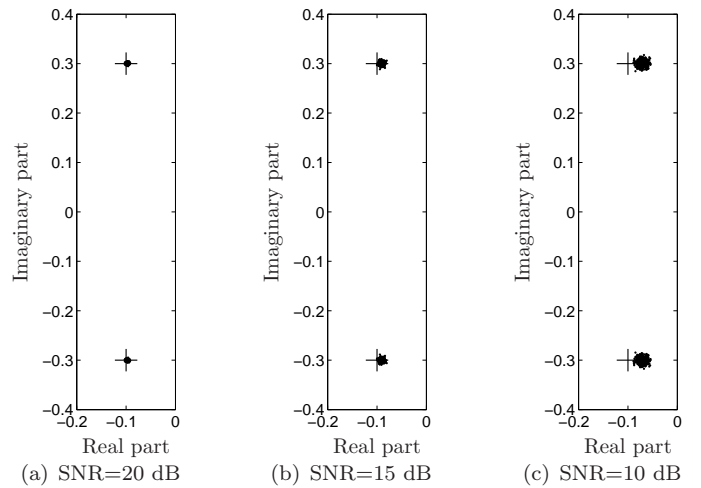


Fig. 4. Estimated poles over 500 runs for various SNRs, where + denotes the true poles ( $\alpha$  known)

Table 2. Normalized MSE of poles ( $\alpha$  known).

SNR=20 dB	$-0.0676 \cdot 10^{-4} \pm i 0.3257 \cdot 10^{-4}$
SNR=15 dB	$-0.0684 \cdot 10^{-3} \pm i 0.2475 \cdot 10^{-3}$
SNR=10 dB	$-0.0834 \cdot 10^{-2} \pm i 0.2665 \cdot 10^{-2}$

## 5. FRACTIONAL ORDER ESTIMATION

In this section, we assume that the fractional derivative order  $\alpha \in ]0, 2[$  is unknown and has to be estimated by minimizing a quadratic criterion:

$$\hat{\alpha} = \arg \min_{\alpha \in ]0, 2[} \frac{1}{2} \|\hat{y}_c(\alpha) - y_c\|_2^2, \quad (21)$$

where  $y_c$  is the vector (of length  $pN$ ) resulting from the concatenation of the  $p$  system outputs and  $\hat{y}_c(\alpha)$  is the vector resulting from the concatenation of the  $p$  outputs estimated with the MOESP method presented in section 3 for a given  $\alpha$ . The value of  $\alpha$  in (21) is obtained through a nonlinear optimization technique. The iterative algorithm used is based on a subspace trust-region method and on the interior-reflective Newton method. As a consequence, the proposed MOESP algorithm is executed at each iteration of the optimization technique. The number of state variables  $n$  is assumed to be known.

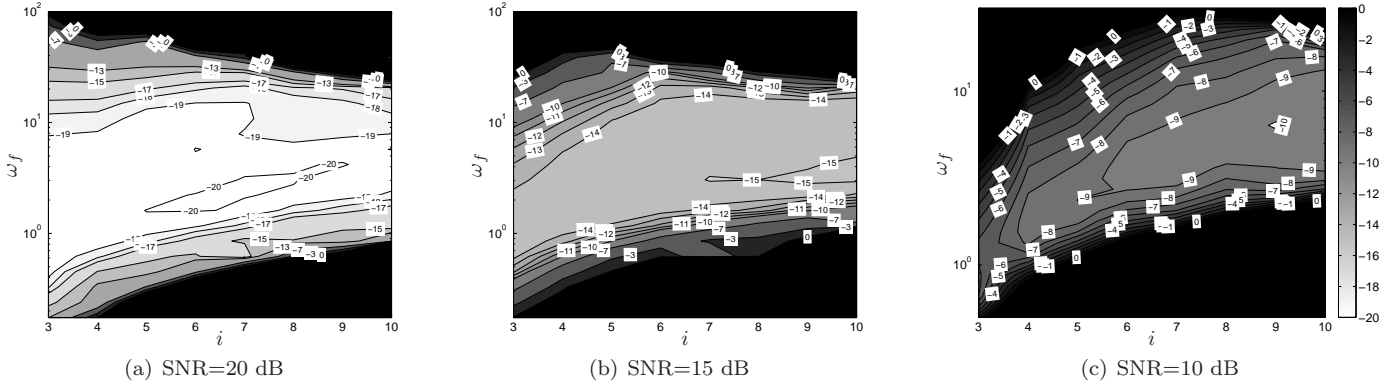


Fig. 3. Normalized error norm  $\|\hat{y} - y\|_2/\|y\|_2$  in dB versus the number of block rows  $i$  and the filter frequency  $\omega_f$  for various SNRs.

This method is applied on the same data set used in the first example, with SNR=20 dB. The algorithm parameters are also the same. The estimation results are:

$$\hat{A} = \begin{bmatrix} 0 & -0.1008 \\ 1 & -0.1757 \end{bmatrix}, \hat{B} = \begin{bmatrix} 1 \\ 0 \end{bmatrix}, \hat{\alpha} = 0.8894,$$

$$\hat{C} = \begin{bmatrix} 0.0012 & 0.1012 \\ 0.4997 & -0.0923 \end{bmatrix}, \hat{D} = \begin{bmatrix} 1.3782 \cdot 10^{-3} \\ -0.6763 \cdot 10^{-3} \end{bmatrix}.$$

The normalized prediction error norm is equal to 0.1050 (-19.57 dB) for the first output and 0.1008 (-19.93 dB) for the second one. As expected, the normalized errors obtained here are better than those obtained in the previous section for  $\alpha$  fixed to its true value because  $\alpha$  is optimized so as to minimize the prediction error. In Fig. 5, the criterion to be minimized to estimate the commensurate order  $\alpha$  is plotted. We observe that the minimum can be easily reached by the optimization algorithm.

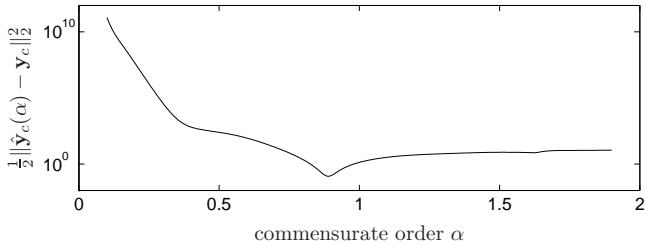


Fig. 5. Criterion to minimize with respect to  $\alpha$  for a data set with SNR=20 dB (true commensurate order: 0.9)

Now, in the context of commensurate order optimization, we present results obtained using a Monte Carlo simulation with 500 runs for three values of the SNR (20, 15 and 10 dB). The histograms of the estimated order  $\alpha$  are given in Fig. 6. We observe a bias which increases with the noise level. This is obviously due to the bias introduced by the MOESP algorithm. Table 3 gives the means of the normalized error norms. Again, they are slightly better than the ones obtained in table 1 when  $\alpha$  is fixed to its true value. Nevertheless, concerning the estimates of the poles, the previous results are better than those obtained here (see Fig. 7). Indeed, the normalized MSEs of the poles presented in table 4 are larger than the ones in table 2. Note that similar results are obtained by considering systems with an other commensurate order.

Table 3. Means of the normalized error norms over 500 runs ( $\alpha$  estimated).

	output	SNR=20 dB	SNR=15 dB	SNR=10 dB
mean of the normalized error norm	1	0.1026 (-19.78 dB)	0.1834 (-14.73 dB)	0.3327 (-9.56 dB)
	2	0.1005 (-19.95 dB)	0.1797 (-14.91 dB)	0.3282 (-9.68 dB)

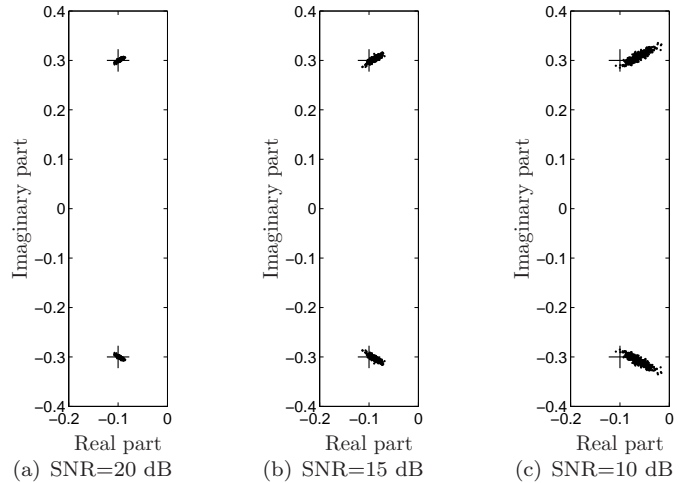


Fig. 7. Estimated poles over 500 runs for various SNRs, where + denotes the true poles ( $\alpha$  estimated)

Table 4. Normalized MSE of poles.

SNR=20 dB	$-0.4952 \cdot 10^{-4} \pm i 0.8875 \cdot 10^{-4}$
SNR=15 dB	$-0.2530 \cdot 10^{-3} \pm i 0.6315 \cdot 10^{-3}$
SNR=10 dB	$-0.1208 \cdot 10^{-2} \pm i 0.5740 \cdot 10^{-2}$

## 6. CONCLUSION

This paper focuses on the identification of CT systems using fractional state-space models. Thanks to an adapted data filtering, we have shown that subspace-based algorithms can be used to estimate the state-space matrices. Simulation results have shown that the estimation results are not very sensitive to small variations of the tuning parameters. The commensurate differentiation order is estimated by using nonlinear programming. Simulation examples have shown that the estimators are biased. So, a

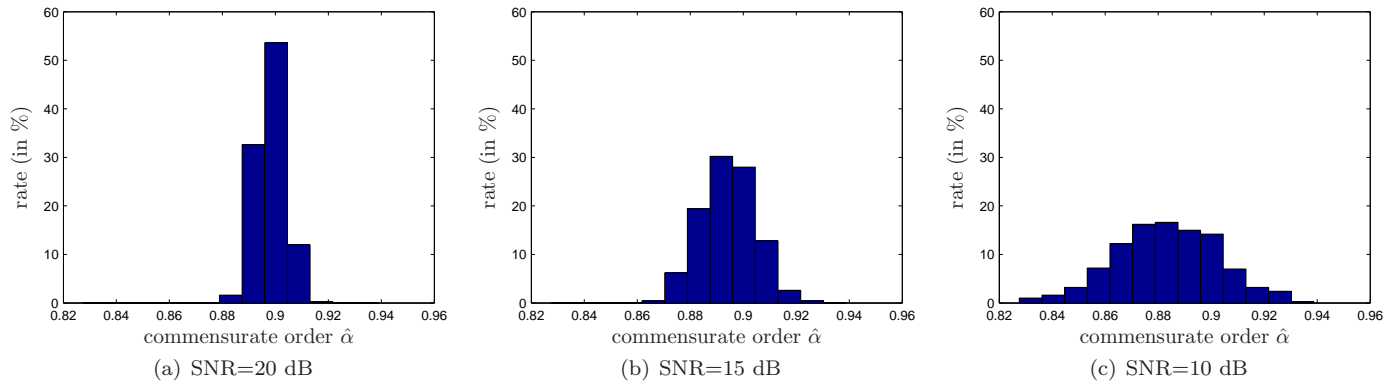


Fig. 6. Histograms of the estimated commensurate order  $\alpha$  for various SNRs

future work consists in developing stochastic methods to eliminate this bias.

## REFERENCES

- M. Aoun, R. Malti, F. Levron, and A. Oustaloup. Numerical simulations of fractional systems: an overview of existing methods and improvements. *Nonlinear Dynamics*, 38:117–131, 2004.
- M. Aoun, R. Malti, F. Levron, and A. Oustaloup. Synthesis of fractional Laguerre basis for system approximation. *Automatica*, 43(9):1640–1648, September 2007.
- T. Bastogne, H. Garnier, and P. Sibille. A PMF-based subspace method for continuous-time model identification. application to a multivariable winding process. *Int. J. Control*, 74(2):118–132, 2001.
- J.-L. Battaglia, O. Cois, L. Puigsegur, and A. Oustaloup. Solving an inverse heat conduction problem using a non-integer identified model. *Int. J. Heat Mass Transfer*, 44(14):2671–2680, 2001.
- D. Bauer. Order estimation for subspace methods. *Automatica*, 37:1561–1573, 2001.
- D. Bauer and M. Jansson. Analysis of the asymptotic properties of the MOESP type of subspace algorithms. *Automatica*, 36:497–509, 2000.
- O. Cois, A. Oustaloup, T. Poinot, and J.-L. Battaglia. Fractional state variable filter for system identification by fractional model. In *Proc. of the European Control Conference*, Porto, Portugal, Sept. 2001.
- B. R. J. Haverkamp, C. T. Chou, M. Verhaegen, and R. Johansson. Identification of continuous-time MIMO state space models from sampled data, in the presence of process and measurement noise. In *Proc. of the 35th Conference on Decision and Control*, Kobe, Japan, 1996.
- R. Johansson, M. Verhaegen, and C. T. Chou. Stochastic theory of continuous-time state-space identification. In *Proc. of the 36th Conference on Decision and Control*, San Diego, California, USA, Dec. 1997.
- R. Johansson, M. Verhaegen, and C. T. Chou. Stochastic theory of continuous-time state-space identification. *IEEE Trans. Signal Process.*, 47(1):41–51, 1999.
- T. Katayama. *Subspace methods for system identification*. Springer, 2005.
- R. Malti, S. Victor, and A. Oustaloup. Advances in system identification using fractional models. *J. Comput. Nonlinear Dyn.*, 3(2), January 2008a.
- R. Malti, S. Victor, A. Oustaloup, and H. Garnier. An optimal instrumental variable method for continuous-time fractional model identification. In *Proc. of the 17th IFAC World Congress*, Seoul, South Korea, July 6-12 2008b.
- D. Matignon. Stability properties for generalized fractional differential systems. In *ESAIM : Proceedings, Fractional Differential Systems: Models, Methods and Applications*, volume 5, pages 145–158, 1998.
- D. Matignon and B. d’Andréa Novel. Some results on controllability and observability of finite-dimensional fractional differential systems. In *IEEE-CESA ’96, SMC IMACS Multiconference*, pages 952–956, France, 1996.
- G. Mercère, R. Ouvrard, M. Gilson, and H. Garnier. Subspace based methods for continuous-time model identification of MIMO systems from filtered sampled data. In *Proc. of the European Control Conference*, Kos, Greece, 2007.
- A. Ohsumi, K. Kameyama, and K.-I. Yamaguchi. Subspace identification for continuous-time stochastic systems via distribution-based approach. *Automatica*, 38:63–79, 2002.
- K. B. Oldham and J. Spanier. Diffusive transport to planar, cylindrical and spherical electrodes. *J. Electroanal. Chem. Interfacial Electrochem.*, 41:351–358, 1973.
- K. B. Oldham and J. Spanier. *The Fractional Calculus: Integrations and Differentiations of Arbitrary Order*. Academic Press, New-York, 1974.
- A. Oustaloup. *La dérivation non entière. Théorie, synthèse et applications*. Hermès, Paris, 1995.
- A. Oustaloup, L. Le Lay, and B. Mathieu. Identification of non integer order system in the time-domain. In *IEEE-CESA ’96, SMC IMACS Multiconference*, 1996.
- T. Poinot and J.-C. Trigeassou. Identification of fractional systems using an output-error technique. *Nonlinear Dynamics*, 38(1-2):133–154, 2004.
- J. Sabatier, M. Aoun, A. Oustaloup, G. Grégoire, F. Ragot, and P. Roy. Fractional system identification for lead acid battery state charge estimation. *Signal Processing*, 86(10):2645–2657, 2006.
- S. G. Samko, A. A. Kilbas, and O. I. Marichev. *Fractional Integrals and Derivatives : Theory and Applications*. Gordon and Breach, Yverdon, Switzerland, 1993.
- J.-C. Trigeassou, T. Poinot, J. Lin, A. Oustaloup, and F. Levron. Modeling and identification of a non integer order system. In *Proc. of the European Control Conference*, Karlsruhe, Germany, 1999.